Standardization of NPS Measurement: Interim Report of AAPM TG16

Andrew D. A. Maidment[a], Michael Albert[a], Phillip C. Bunch[b], Ian A. Cunningham[c], James T. Dobbins, III[d], Robert Gagne[e], Robert M. Nishikawa[f], Richard Van Metter[b], Robert F. Wagner[e]

[a]University of Pennsylvania, Philadelphia, PA 19104–4227
[b]Eastman Kodak Corporation, Rochester, NY 14650–2033
[c]University of Western Ontario, London, Ontario, Canada
[d]Duke University, Durham, NC 27710
[e]U.S. Food and Drug Administration, Rockville, MD 20857
[f]University of Chicago, Chicago, IL 60637

ABSTRACT

This article reviews the state of the Noise Power Standard being drafted by Task Group No. 16 for the American Association of Physicists in Medicine. The Standard is intended to represent a consensus on acceptable practices in the measurement and reporting of noise power spectra for digital radiographic imaging devices based on single projections and to contain informative sections which will be of use to those not completely familiar with the measurement and interpretation of noise power spectra. Several of the issues considered by the committee are reviewed, including issues of conditioning and windowing data, issues specific to several modalities, and various methods of data presentation. A note on the historical background of noise power measurements and a brief discussion of possible avenues for future research is included.

Keywords: Noise power spectrum, Wiener spectrum, AAPM, radiography, mammography, digital.

1. INTRODUCTION

The American Association of Physicists in Medicine (AAPM) standard for Noise Power Spectra (NPS) is intended to provide the medical imaging community with a common language in which to discuss NPS measurements, a common set of expectations as to how such measurements are to be made and reported, and to provide enough introductory material so that the document can be a useful introduction to NPS in the context of medical imaging. To this end, the AAPM commissioned Task Group No. 16 in 1996 to review the available literature and produce a document which expounds the relevant theoretical background, details issues of measurement and calculation, and provides reference data sets, with the aim of summarizing issues that affect NPS measurements and assuring a common normalization to such measurements.

The members of Task Group No. 16 were drawn from academic institutions in the United States and Canada, from the U.S. Food and Drug Administration (FDA) and national laboratories, and from industry. Additionally, the Task Group benefited from contributions by academics and industrial representatives of many nations. Informally, the Task Group coordinated its efforts with the continuing work of Committee 62B of the International Electrotechnical Commission (IEC) on the detective quantum efficiency[1,2] (DQE) and appropriate x-ray spectra[3] for such measurements.

The literature on the quality of images formed by a limited number of quanta can be traced back to the classic work of Rose who emphasized the fundamental question of whether a signal could be distinguished from statistical fluctuations or *quantum mottle*. For many systems, in particular silver-halide films with or without the use of an intensifying screen, it has proven useful to study these statistical fluctuations in terms of their

Further author information: Send correspondence to A.D.A.M.: E-mail: maidment@rad.upenn.edu, Telephone: (1 215) 662 6225, Fax: (1 215) 349 5115, Address: Hospital of the University of Pennsylvania, Department of Radiology, 1 Silverstein, 3400 Spruce Street, Philadelphia, PA 19104

frequency components, thus introducing the concept of a noise power spectrum. By measuring the NPS of an imaging system, and in particular by comparing that measurement to the noise inherent in the statistical fluctuations due to the finite number of primary x-ray quanta, one could determine how efficiently the primary x-rays are used and obtain information about other sources of noise in the imaging system. This information is clearly important in the design of such systems given the competing goals of good image quality and low dose to the patient.

A particularly significant part of the literature for the Task Group was previous efforts at standardizing and codifying the measurement of noise power spectra and related issues, including the work of the International Commission on Radiation Units[4] (ICRU) and the FDA.[5] The introduction of digital imaging systems, characterized by a discrete set of sample points at each of which a measurement is recorded as one of a finite set of levels and by the general availability of the resulting data for use with modern computers, has introduced several conceptual and practical issues which have not been previously addressed by a standard. The task group therefore addressed issues ranging from how the x-ray spectra used in measuring the NPS should be specified, to what processing might be done to the digital data, to the very definition of the NPS for digital systems. A brief overview of these efforts is discussed in this paper, while more details and references can be found in the Standard itself.

2. BACKGROUND

As Heraclitus[6] observed that one can not cross the same river twice, it can similarly be asserted that one can never acquire the same image twice. Each realization of the imaging process will be subject to random fluctuations. One unavoidable source of this noise is the random fluctuations in the primary x-ray flux and the probabilistic nature of the primary interactions of the x rays with the detector. Furthermore, each stage in the imaging process that involves the production of new quanta, such as the production of visible light photons or the promotion of electrons into the conduction bands of semi-conductors, constitutes another source of noise. A variety of additional sources of noise, such as electronic noise or shot noise, will also degrade the quality of the final image. These random fluctuations place fundamental limits on the reliability with which one can distinguish the weakest signals of interest from the background. From the point of view of clinicians, an image with significant quantum mottle appears *grainy*, and clinically significant lesions can be obscured or non-existent lesions can be mistakenly identified.

The experimental measurement of noise in projection radiography can be traced back to the work of Sturm and Morgan,[7] while in later work by multiple researchers[8–13] the ideas of spectral analysis were introduced. Early measurements of the NPS of radiographic films were performed using analog devices in which the film, mounted on a rotating cylinder, was moved past an illuminated slit so that the intensity of light passing through the film could be monitored by an analog electronic spectrum analyzer. Later, scanning digital microdensitometers were introduced. The question of absolute calibration for film was solved in terms of standardized diffuse density[5,14] and it became possible to compare spectra measured by different laboratories[14,15] and techniques.

The application of spectral techniques to radiographic film has been particularly fruitful because film, under appropriate conditions, approximately satisfies the assumptions of stationarity and linearity upon which the theory of signal detection for linear systems is based. A system is said to be stationary if its response to a signal is independent of position relative to the device. A system is said to be linear if a change in the incident signal results in a proportionate change in expected value of the record of that signal. For the purposes of noise power spectra, the condition of stationarity is not strictly necessary, but can be replaced by the weaker condition of *wide-sense* stationarity. A system is said to be wide-sense stationary if its second–order statistics, *i.e.* its autocorrelation function, are independent of position relative to the detector. For small variations relative to a uniform x-ray exposure, radiographic films approximately satisfy both conditions. In terms of stationarity in particular, the response of appropriately manufactured film does not depend upon position unless one considers length scales so small that the discrete nature of the silver–halide crystals becomes apparent or length scales as large as the film sheet itself.

The introduction of storage phosphors and computed radiography in the 1980s made issues related to the NPS of digital systems[16–18] matters of immediate concern to the medical physics community. It should be noted that storage phosphors are, in many ways, intermediate between analog systems and fully digital systems. In particular, the storage phosphor itself is an analog device and under ideal circumstances would be a truly stationary device, while the read-out introduces discrete sampling in much the manner that a film densitometer will discretely sample an array of positions on a piece of film. More recently introduced technologies such as flat panel devices are intrinsically digital, and the nature and spacing of the sample points are intrinsically part of the detector.

As digital detectors produce arrays of discretely spaced samples, and the sample spacing is generally not much smaller than the smallest objects of clinical interest, these detectors can no longer be considered strictly stationary. Thus, for an object of a size similar to or smaller than the spacing between sample points, the detectability of such an object will in general vary if the object is moved by a fraction of the sample spacing. However, if the object is moved by an integer multiple of the sample spacing (along either axis), then ideally the detectability of the object should not change. A system is said to be *cyclo–stationary* if moving an integer multiple of the sample spacing does not change the the expected recorded signal, and *wide-sense cyclo–stationary* if the second–order statistics do not change between two positions separated by an integer multiple of the sample spacing. Using this weaker condition one can develop a theory for digital detectors[19–24] from several perspectives which is in many ways analogous to the theory of detectors that demonstrate true stationarity.

3. CONTENTS OF THE STANDARD

The contents of the standard attempt to serve several purposes and are addressed to several audiences. A significant amount of background material is included which is intended to help individuals previously unfamiliar with the measurement or interpretation of noise power spectra, including a glossary, a review of the the meaning of the NPS under ideal circumstances, and a brief historical summary containing references to the literature which will serve as a starting point for more exhaustive study. Several sample data sets and sample software are provided for the convenience of those performing NPS measurements as a starting point and in particular to help avoid errors in the normalization of reported results.

Perhaps most importantly, the Standard discusses a large number of issues which must be addressed by those making noise power measurements so that their data can be interpreted and compared to the results of other workers. For example, researchers must indicate the quality of the x-ray beam used and the exposure. Minimally, this would be done by stating the kVp, half–value layer, and a measurement of the exposure. Preferably, researchers should report the NPS corresponding to an x–ray spectrum identified by the relevant IEC standard.[3] Further, researchers should report the NPS at a beam quality and exposure, or a range of qualities and exposures, which are similar to those that would generally be encountered given the proposed clinical use of the device. Note that, as at many other points in the standard, researchers can report data measured under conditions which are not clinically relevant as such information might be of scientific or engineering interest, but such measurements must be clearly labeled as not being representative of the device when used as intended for diagnostic imaging. The standard also makes several suggestions as to how researchers might present their data.

The use of digital detectors in conjunction with modern computers permits a wide variety of corrections and adjustments to be applied to the raw measurements produced by the individual detector elements. Some of these, such as routine linearity calibrations based on "flat field" and "dark field" images, should be applied to data used for measurements of the NPS in the same manner as applied to diagnostic images, as this best represents the diagnostic capability of the device. On the other hand measurements of the NPS based on "common mode rejection," *i.e.* subtracting two images acquired serially so as to remove any persistent structure, is not considered representative of the diagnostic capabilities of the system. The use of common mode rejection can significantly underestimate the NPS of devices that show certain effects such as ghosting or lag where after–images cause correlation between successive images. While common mode rejection is often useful for answering questions of interest to the physicist or engineer, any NPS measured using this technique must be clearly labeled as not necessarily representative of the diagnostic capabilities of the system in a clinical setting. The standard requires that researchers presenting a NPS explicitly clarify a number of similar issues, and simultaneously provides a common vocabulary for this purpose.

Actual imaging devices do not behave ideally, and this deviation from ideal behavior varies between modalities. The standard attempts to explicitly discuss what corrections should be applied so that the resulting measurements are clinically relevant, and discuss what corrections would be misleading if the resulting NPS were presented as representative of the clinical efficacy of the detector. For example, corrections to remove non-uniformities in the incident x-ray beam by fitting flat–fields to low–order polynomials are reasonable, although researchers must explicitly state the nature of these corrections. On the other hand, calibration of individual photostimulable–phosphor plates is generally considered unacceptable for a NPS measurement which is presented as representative of the clinical efficacy of a CR product, as no system for calibrating and tracking individual plates has shown to be practical in a clinical setting.

The standard is intended to be of use for all digital imaging systems which acquire single projection images. In particular, fluoroscopy is not treated as the multiple frames acquired are not independent and the resulting time and space correlations are a topic in need of further research. The standard is intended to apply to both general radiography and mammography, whether implemented using technologies such as structured cesium iodide or amorphous selenium, implemented using a photo–stimulable phosphor, or implemented by digitization of radiographic film.

4. BEST PRACTICES

Given the diversity of diagnostic imaging equipment currently used or contemplated, it is not possible to completely prescribe all details that must be addressed in order to make a NPS measurement which will be useful and reliable. Acknowledging this limitation, the standard attempts to systematize the current experience of the medical imaging community. Some issues apply to all detectors, such as the advantages and disadvantages of using non-trivial windows (*i.e.* other that "rect " functions) or the various compromises one can make in terms of decreasing the statistical uncertainty in the estimate of the NPS at the cost of decreasing the spectral resolution.

4.1. Windowing

Windowing is an attempt to remove artifacts in the NPS due to the finite data length used to calculate the NPS but is frequently misused. As an example, consider a simulation of a one–dimensional detector, assuming Gaussian statistics with an NPS as shown by the thick line in Fig 1a. This NPS was chosen to have a large, narrow peak at 1/3 of the detector pitch. The thinner solid lines show the NPS calculated using samples of lengths 16, 128, and 1024 detector elements, averaged over 10^4 simulations. Each of these three calculated spectra show an artifact known as "spectral leakage", in which the power in the sharp peak is smeared out across the spectrum. Qualitatively, the finite Fourier transform implicitly imposes periodic boundary conditions, resulting in an apparent discontinuity at the end-points if there are frequencies present that do not correspond to a whole number of cycles over the length of the sample. Quantitatively, the calculated spectrum is a convolution of the true spectrum and a function determined by the window used. For the three solid curves, the "window" used was a trivial *rect* window. The solid line in Fig 1a labeled "16" represents the convolution of the true spectrum with the first of the curves shown in Fig. 1b. It is clear that as the sample length increases, the calculated NPS approaches the actual NPS, and this is also seen in Fig. 1b where the *rect* window corresponding to a 128 samples length has less power in the "wings" at either side of the central peak than the window for a length of 16. The dashed curves in Fig. 1a represents the same calculations but using a window, *i.e.* the simulated detector data is first multiplied by a function which vanishes smoothly at the endpoints of the sample region (here, a Hann window was used). The results shown by the dashed curves in Fig 1a show a significant reduction in spectral leakage for only modest increases in the length of the data sample. Indeed, the curve corresponding to a windowed sample 1024 element long is indistinguishable from the thick line in Fig 1a. The same fact can be seen in Fourier space in Fig 1b where the function corresponding to a Hann window for a sample 16 elements long is seen to decrease relatively quickly away from the central peak. Thus, the use of a window such as the Hann window allows, in certain cases, the use of shorter sample lengths. In addition to being a calculational convenience, this allows greater flexibility is choosing regions of the detector away from artifacts such as seams and in choosing a region of the detector sufficiently small so that the requirement of stationarity is satisfied to a reasonable degree.

Non-trivial (that is, non-*rect*) windows, however, are of limited use in the practical measurement of the NPS for several reasons. First, sharp peaks at non-zero frequencies such as that shown in the simulation are relatively rarely encountered. When sharp peaks at non-zero frequencies are encountered, they often are better interpreted

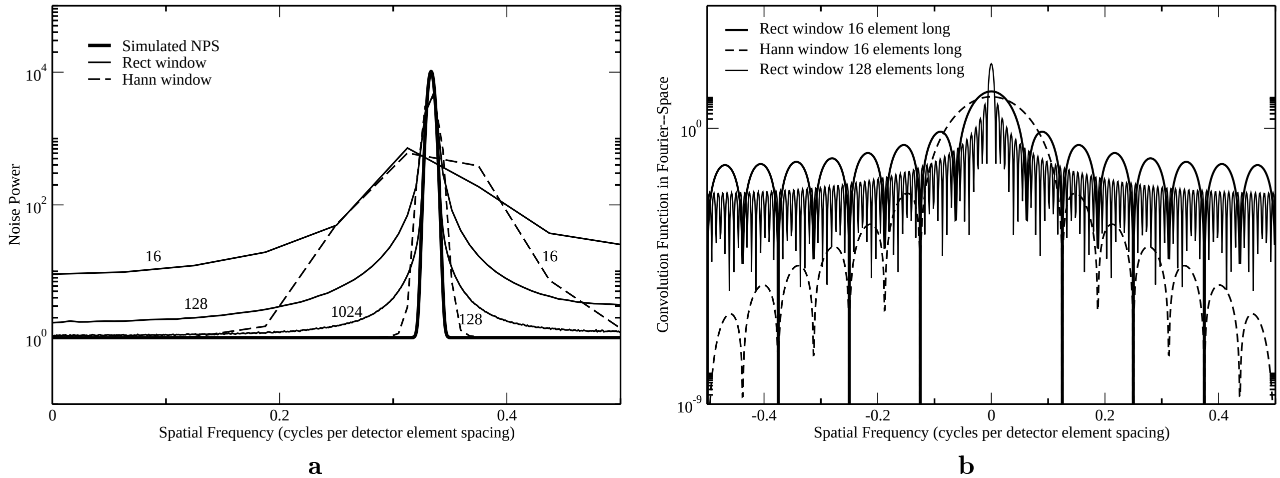

Figure 1. Part a: simulation of a one dimensional detector, showing the actual NPS used to generate the simulated data (thick line), spectra calculated using data sets 16, 128, and 1024 data elements long (solid lines) with a trivial *rect* window, and spectra calculated using a Hann window on samples of lengths 16 and 128. Part b: These functions convolved with the actual spectrum from Part a give the measured noise spectra for the three cases corresponding to a *rect* window 16 long, a Hann window *16 long*, and a *rect* window 128 elements long. In part b, some of the vertical asymptotes towards $\log(0) = -\infty$ have been left truncated as this reduces visual clutter.

not as noise but as artifacts. Often, these can be traced back to electronic sources whose frequencies are precisely matched to the readout and thus would not "leak." For example, if a CCD were designed to alternate between two analog–to–digital converters, any discrepancy in the behavior of these converters would show up as a sharp peak of frequency 0.5 times the detector pitch. As the NPS is usually calculated using samples of even length, this frequency would not leak. Additionally, while the wings of the *rect* function are relatively large, the zeros occur at precisely integer multiples of the reciprocal of the sample length. This is important as essentially all detectors show a large amount of noise power in the zero–frequency bin due to instability of the x–ray source between exposures. Windows other than the *rect* function will generally not have their zeros in these positions and thus will allow this very large source of noise to dominate the entire spectrum. Note, for example, the Hann window for 16–elements in Fig. 1b does not have zeros at $\pm 1/16$ of the detector pitch. Also, note that the central lobe of the Hann window is somewhat wider than that of the *rect* function for the same sample length, although the side lobes of the Hann window fall off faster. Thus the use of a window requires *a priori* knowledge of what one expects to reasonably find in the NPS, and a large number of windows have been designed and studied.[25] In general, for the measurement of the NPS, the *rect* window and the Hann window are sufficient for most circumstances.

4.2. Data Display

The display of the NPS as a function of spatial frequency along both axes presents additional problems which can be addressed by a variety of methods, several of which are illustrated in Fig. 2 for simulated data calculated on regions which are 64 times the detector spacing on each side. Fig. 2a shows a two dimensional histogram in which the height of each bin corresponds to the NPS at a given frequency along the x and y-axes. This display method allows the simultaneous presentation of the entire data set. Particularly useful, given appropriate computer software, is the ability to interactively adjust such features as the range of spatial-frequencies displayed and the angle from which the two dimensional histogram is viewed. Here one quadrant of frequency space is displayed.

Fig. 2b shows a more conventional presentation of NPS data by graphing slices through the two dimensional NPS and the angular average as a function of a single frequency variable. A significant advantage of this method is that the actual data can be recovered by the reader with fairly good accuracy. However, slices through the data can be misleading. Many detectors, such at the one simulated here for illustration, show peaks in the

NPS near the natural axes of the system. Thus, if only the data along the horizontal and vertical axes were presented, the NPS of the system would be over–estimated for most purposes. Also, note that for the 45° curve, the data is plotted out to $1/\sqrt{2} \approx 0.707$ times the detector pitch, corresponding to the components of spatial frequency on each axis simultaneously achieving a maximum of 0.5 times the detector pitch. This increased range of response corresponds to the actual behavior of such devices, and can be observed in many systems by comparing images of a line–pair phantom with the lines parallel to the axes of the detector and images with the lines on the diagonal. Not all detectors will demonstrate this, particularly if the modulation transfer function (MTF) has been engineered to remove aliasing (response to spatial frequencies greater than the sampling pitch). In either case, data at these frequencies represents part of the actual behavior of the imaging device and can not be ignored *a priori*, although in general they should represent regions of frequency space containing relatively little noise power.

Parts (c) and (d) of Fig. 2 represent the NPS in terms of a contour plot and a gray scale image. These plots show the full two dimensional data set, but unlike two dimensional histograms (or similar methods such as surface plots) there are no problems of attempting to suggest a sense of visual perspective. Contour plots allow for quantitative reading, but if multiple contours are shown corresponding to small increments of the NPS, such plots can become difficult to read. Gray scale plots have the advantage that one does not need to choose a small set of levels corresponding to contours. However, it is generally more difficult to view a gray scale image quantitatively. One could provide a calibrated scale as a legend, but accuracy is limited by the nature of the printing processes and the ability of the viewer to distinguish shades of gray. One could also code ranges of NPS values in terms of colors as on a "heat" scale, but one faces additional issues such as the cost of color printing and the various types of color–blindness which are not uncommon. Both the contour plot and the gray scale plot illustrate that the zero–spatial–frequency point of the NPS is a point of symmetry, *i.e.*, $\mathrm{NPS}(-u,-v) = \mathrm{NPS}(u,v)$. Thus one could choose to display one half of either figure. The apparent reflection symmetries about the detector axes (*i.e.*, $\mathrm{NPS}(-u,v) \approx \mathrm{NPS}(u,v)$ and $\mathrm{NPS}(u,-v) \approx \mathrm{NPS}(u,v)$, result from the choice of the NPS used to simulate this data, and can not be assumed *a priori*, but must be experimentally tested. Of course any appreciable asymmetry of the NPS with respect to reflection about either axis would be of interest in understanding an imaging device, and in particular when such asymmetries occur extra care must be taken so that the axes presented graphically can associated with the physical axes of the imaging device.

No one method of presenting two dimensional NPS data can serve in all situations. A variety of methods of presentation allow multiple aspects of the NPS to be visualized, and thus the method of presentation will be in part influenced by the what aspects of the NPS one wishes to discuss. It is worth noting that a variety of freely-distributed software packages can be used in producing graphical representations such as those in Fig. 2. In particular, the two–dimensional histogram was produced using software based on a widget set available[26] from the Fermi National Laboratory, the graph in Fig. 2b was produced using *Grace*,[27] and the contour plot and gray–scale image were produced with *Scilab*.[28]

4.3. Specific Modalities

In general it is necessary to consider the nature of each specific modality in order to produce a useful NPS measurement. For example, CR systems present several distinctive features[17,29,30] which must be taken into account. Experience has shown that the NPS of CR systems is significantly different in the *scan* and *sub-scan* directions (the scan direction corresponds to the continuous readout of a line of data and the sub-scan direction is perpendicular to this), thus necessitating the measurement of the full two dimensional (2D) NPS. Further, examination of the 2D NPS has been found to show that the NPS peaks along the two axes so that one dimensional (1D) NPS measurements could be misleading by demonstrating substantial noise capable of masking diagnostic signals. However, as a practical matter plots of 1D NPS measurements are often desirable when communicating research results. The standard, while encouraging the presentation of the full 2D NPS, discusses several appropriate ways to reduce the 2D NPS spectra to 1D plots for convenient display.

To make clear the need to understand the peculiarities of each modality, it is instructive to turn to the case of digitized radiographic films. For radiographic film great care must be exercised in linearizing with respect to the standard ISO[31] diffuse optical density or transmittance, a calibration which must be performed for each brand of film and each allotment. Also, film is subject to a variety of artifacts, many of which are introduced

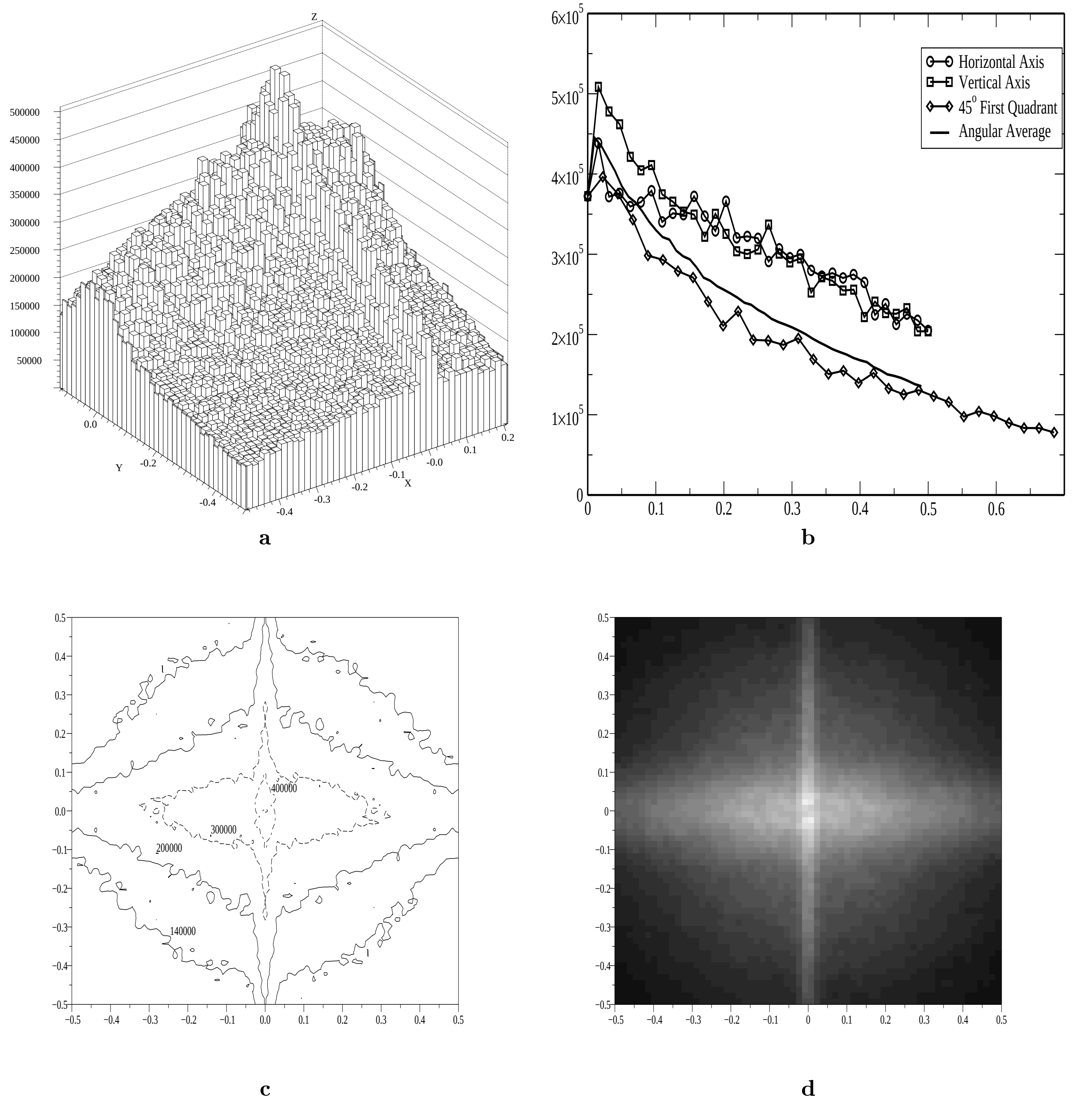

Figure 2. Several methods of displaying NPS data: (a) a two dimensional histogram; (b) slices and the radial average; (c) a contour plot; (d) a gray scale image.

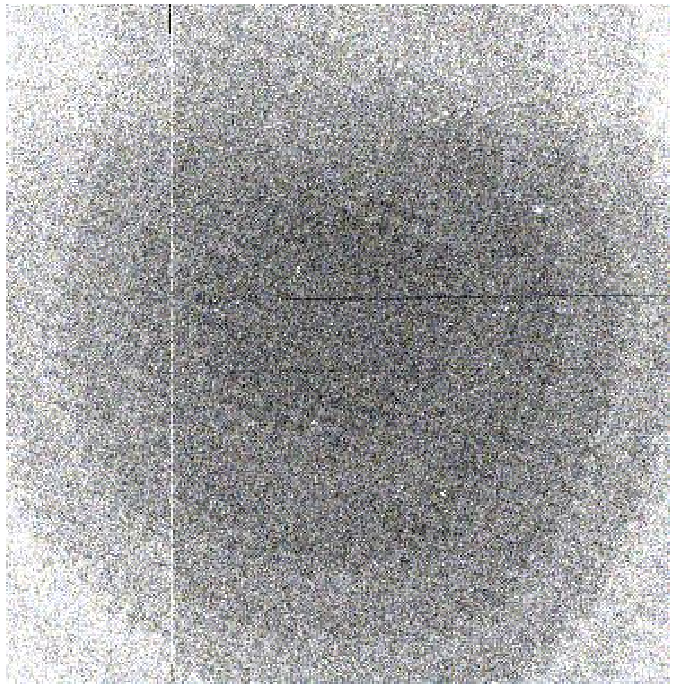

Figure 3. Variation in noise between detector elements for a detector using a fiber–optic coupled CCD. Gray scales represent the standard deviation among values reported by individual detector elements across multiple exposures.

by the development process. While these artifacts degrade the quality of images, it is generally not useful to try to quantify these effects in terms of the NPS. Thus, only films which are essentially devoid of artifacts should be used for NPS measurements. Additionally, the experimenter working with film must explicitly distinguish between measurements characterizing the film itself or measurements characterizing the film as digitized using a specific technology. If the aim is to characterize the film itself, then effects related to the digitization process must be explicitly dealt with, either by demonstrating that the effects of digitization have not significantly changed the resulting NPS or by correcting for the digitization process. In making corrections for digitization, researchers must be particularly aware of the effects of the scanning aperture, the possibility of aliasing effects which will result in high–frequency noise on the film being added to the measured low–frequency noise of the digitized image, and any additional sources of noise intrinsic to the digitizer. In general, digitizers adequate for clinical use have not shown themselves adequate for measuring the properties of the film proper.

5. FUTURE RESEARCH

While the NPS is now a customary part of the quantitative assessment of imaging technologies, and it is hoped that the Standard will increase the utility of such measurements, it should be noted that there are many topics which might be profitably researched. Computed tomography (CT), magnetic resonance imaging (MRI), and ultrasound were explicitly beyond the scope of the current work, as was any form of time–sequential image acquisition such as fluoroscopy.

At a fundamental level, it must be noted that real systems often do not ideally satisfy the conditions of stationarity or cyclo-stationarity on which the NPS is based. For example, Fig. 3 was produced with a digital x-ray imaging system by calculating the standard deviation of the digital values reported by individual detector elements over multiple exposures. For an ideal, stationary or cyclo-stationary detector, such an image would appear as a flat field with only random variations. Instead, this detector shows evidence of several levels of structure related to the construction of the detector. This particular device consisted of a CCD coupled to an fiber–optical taper. The series of concentric circles is presumably related to relative efficiency with which light is collected in various regions. While routine calibration sets the gains in individual detector elements so that flat fields appear flat, the efficiency with which light is collected for the various detector elements is still seen in the statistical properties of the image. Although it is harder to discern, there is also a cross-hatched or "chicken–wire" effect which again is presumably related to the fiber-optic structure. How this effects the NPS, how this effects the detectability of clinically relevant signals, or how the NPS might be measured so as to best represent the ability of the device to detect clinically relevant signals, are all open questions. Indeed, considerations such as these have led some researchers[32,33] to consider rejecting the NPS in favor of non-spectral measures.

Looking farther into the future, it must be noted that there are possibly useful technologies which make use of the physical properties of x–rays beyond integrating an attenuated x-ray beam. These include systems based on phase–contrast, coherent scatter, and imaging devices that can record individual x-ray interactions and can simultaneously record position and energy information. For such devices, it would seem necessary to develop a framework which moves beyond our current understanding of the NPS to include uncertainties in energy resolution and other effects. It is desirable for such measures, like the NPS, to be connected with the fundamental limits on the ability of a detector to recognize and distinguish various signals or classes of signals.

6. CONCLUSION

The AAPM Noise Power Standard is intended to represent a consensus of the medical imaging community on the basic methods of measuring the spectral properties of the noise of imaging systems. The standard also provides introductory material and sample data sets and code as an aide for those who are new to the measurement and interpretation of noise power spectra.

The Task Group has taken advantage of multiple opportunities to ensure that the final document represents an international consensus. In addition to a number of individuals from several continents who have commented to the committee, the working drafts and some related material of the Task Group have been regularly made available to approximately fifty interested parties from around the globe. Additionally, the Task Group has made consistency with other standards a priority, particularly consistency with the work on DQE by Working Group 33 of Committee 62B of the IEC.

As of the writing of this article, the Task Group is completing the draft of the Standard. Once agreement between the standard and the IEC can be assured, the Task Group will report back to the AAPM Diagnostic Committee. Assuming acceptance by the Diagnostic Committee, the draft standard will then be reviewed by the AAPM Science Council. Once both the Committee and the Council are satisfied, the Standard will published by *Medical Physics*, following customary editorial procedures, thus assuring the wide availability of the standard as a reference for future work.

REFERENCES

1. Committee 62B, International Electromechanical Commission, *IEC 61262-5 Ed. 1.0 Medical electrical equipment–Characteristics of electro–optical X-ray intensifiers– Part.5 Determination of the detective quantum efficiency*, 1994.
2. Working Group 33, Committee 62B, International Electromechanical Commission, *IEC 62220-1 Ed.1: Medical electrical equipment – Characteristics of digital X-ray imaging devices – Determination of the detective quantum efficiency.* 62B/477/CDV.
3. Committee 62B, International Electromechanical Commission, *IEC 61267 Ed. 1.0 Medical diagnostic X-ray equipment – Radiation conditions for use in the determination of characteristics.* 62B(C.O.)122 /RV D.
4. International Committe on Radiation Units, Bethesda, Maryland, *ICRU Report 54 Medical Imaging – The Assessment of Image Quality*, 1996.
5. K. Doi, G. Holje, L.-N. Loo, H.-P. Chan, J. Sandrik, R. Jennings, and R. Wagner, *MTFs and Wiener Spectra of Radiographic Screen–Film Systems*, April 1982. FDA 82-8187.
6. Plato, *Cratylus*, vol. 402A.
7. R. E. Sturm and R. H. Morgan, "Screen intensification systems and their limitations," *Am. J. Roentgenology* **62**, pp. 617–634, 1949.

8. E. C. Doerner, "Wiener spectrum analysis of photographic granularity," *J. Opt. Soc. Am.* **52**, pp. 669–672, 1962.
9. K. Doi, "Wiener spectrum analysis of quantum statistical fluctuations and other noise sources in radiography," in *Television in Diagnostic Radiology*, R. Moseley and J. H. Rust, eds., pp. 313–333, Aesculapius, Birmingham, Alabama, 1969.
10. K. Rossmann, "Modulation transfer function of radiographic systems using fluorescent screens," *J. Opt. Soc. Am.* **52**, pp. 774–777, 1962.
11. K. Rossmann, "Measurement of the modulation transfer function of radiographic systems containing fluorescent screens," *Phys. Med. Biol.* **9**, pp. 551–557, 1964.
12. G. Lubberts, "Random noise produced by x-ray fluorescent screens," *J. Opt. Soc. Am.* **58**, pp. 1475–1483, 1968.
13. C. J. Vyborny, L.-N. Loo, and K. Doi, "The energy dependent behavoir of noise wiener spectra in their low-frequency limits: Comparison with simple theory," *Radiology* **144**, pp. 619–622, 1982.
14. J. M. Sandrik, R. F. Wagner, and K. M. Hanson, "Radiographic screen-film noise power spectrum: Calibration and intercomparison," *Appl. Opt.* **21**, pp. 3597–3601, 1982.
15. R. Wagner and J. Sandrik, "An introduction to digital noise analysis," in *The Physics of Medical Imaging: Recording System Measurements and Techniques*, A. G. Haus, ed., pp. 524–545, American Institute of Physics, (New York), 1979.
16. M. L. Giger, K. Doi, and C. Metz, "Investigation of basic imaging properties in digital radiography: 2. Noise Wiener spectrum," *Med. Phys.* **11**, pp. 797–805, 1984.
17. J. T. Dobbins III *et al.*, "DQE(f) of four generations of computed radiography acquisition devices," *Med. Phys.* **22**, pp. 1581–1593, 1995.
18. M. J. Flynn and E. Samei, "Experimental comparison of noise and resolution for 2k and 4k storage phosphor radiography systems," *Med. Phys.* **26**(8), pp. 1612–1623, 1999.
19. M. Giger and K. Doi, *Analysis of MTFs , Wiener Spectra, and Signal–to–Noise Ratios of Digital Radiographic Imaging Systems*, pp. 60–81. AAPM, New York, 1985.
20. I. A. Cunningham, "Applied linear–systems theory," in *Handbook of Medical Imaging, Vol. 1*, J. Beutel, H. Kundel, and R. V. Metter, eds., pp. 79–159, SPIE, (Bellingham, Washington), 2000.
21. A. Papoulis, *Probability, Random Variables, and Stochastic Processes*, McGraw-Hill Inc, 3rd ed., 1991.
22. W. A. Gardner and L. E. Franks, "Characterization of cyclostationary random signal processes," *IEEE Trans. on Info. Theory* **IT-21**, pp. 4–14, January 1975.
23. A. Oppenheim, R. Schafer, and J. Buck, *Discrete Time Signal Processing*, Prentice Hall, Upper Saddle River, New Jersey, 2nd ed., 1999.
24. M. Albert and A. D. A. Maidment, "Linear response theory for detectors consisting of discrete arrays," *Med. Phys.* **27**, pp. 2417–2434, October 2000.
25. F. J. Harris, "On the use of windows for harmonic analysis with the discrete fourier transform," *Proc. IEEE* **66**, pp. 51–83, Jan. 1978.
26. M. Edel *et al.*, *Histo–Scope Plotting Widget Set*, http://www-pat.fnal.gov/nirvana/plot_wid.html, 1998.
27. *Grace*, http://plasma-gate.weizmann.ac.il/Grace/, 2003.
28. INRIA, *Scilab*, http://www-rocq.inria.fr/scilab/.
29. C. D. Bradford, W. W. Peppler, and J. T. Dobbins III, "Performance characteristics of a Kodak computed radiography system," *Med. Phys.* **26**, pp. 27–37, January 1999.
30. E. Samei and M. J. Flynn, "Physical measures of image quality in photostimulable phosphor radiographic systems," *Proc. SPIE* **3032**, pp. 328–338, February 1997.
31. ISO, *Photography – Density measurements – Part 2: Geometric conditions for transmission density*, no. 5-2, 2001.
32. H. H. Barrett, J. L. Denny, R. F. Wagner, and K. J. Myers, "Objective assessment of image quality. II. Fisher information, Fourier crosstalk, and figures of merit for task performance," *J. Opt. Soc. Am. A* **12**(5), pp. 834–852, May 1995.
33. H. H. Barrett, C. K. Abbey, and E. Clarkson, "Objective assessment of image quality. III. ROC metrics, ideal observers, and likelihood-generating functions," *J. Opt. Soc. Am. A* **15 (6)**, pp. 1520–1535, June 1998.